Monthly Notices of the ROYAL ASTRONOMICAL SOCIETY

MNRAS **467,** 1098–1111 (2017) doi:10.1093/mnras/stx057
Advance Access publication 2017 January 16

The ASAS-SN bright supernova catalogue – II. 2015

T. W.-S. Holoien,[1,2★†] J. S. Brown,[1★] K. Z. Stanek,[1,2★] C. S. Kochanek,[1,2] B. J. Shappee,[3‡] J. L. Prieto,[4,5] Subo Dong,[6] J. Brimacombe,[7] D. W. Bishop,[8] U. Basu,[1,9] J. F. Beacom,[1,2,10] D. Bersier,[11] Ping Chen,[6] A. B. Danilet,[10] E. Falco,[12] D. Godoy-Rivera,[1] N. Goss,[1] G. Pojmanski,[13] G. V. Simonian,[1] D. M. Skowron,[13] Todd A. Thompson,[1,2] P. R. Woźniak,[14] C. G. Ávila,[15] G. Bock,[16] J.-L. G. Carballo,[17] E. Conseil,[18] C. Contreras,[15] I. Cruz,[19] J. M. F. Andújar,[20] Zhen Guo,[6,21] E. Y. Hsiao,[22] S. Kiyota,[23] R. A. Koff,[24] G. Krannich,[25] B. F. Madore,[3] P. Marples,[26] G. Masi,[27] N. Morrell,[15] L. A. G. Monard,[28] J. C. Munoz-Mateos,[29] B. Nicholls,[30] J. Nicolas,[31] R. M. Wagner[1,32] and W. S. Wiethoff[33]

Affiliations are listed at the end of the paper

Accepted 2017 January 9. Received 2017 January 6; in original form 2016 October 10

ABSTRACT

This manuscript presents information for all supernovae discovered by the All-Sky Automated Survey for SuperNovae (ASAS-SN) during 2015, its second full year of operations. The same information is presented for bright ($m_V \leq 17$), spectroscopically confirmed supernovae discovered by other sources in 2015. As with the first ASAS-SN bright supernova catalogue, we also present redshifts and near-ultraviolet through infrared magnitudes for all supernova host galaxies in both samples. Combined with our previous catalogue, this work comprises a complete catalogue of 455 supernovae from multiple professional and amateur sources, allowing for population studies that were previously impossible. This is the second of a series of yearly papers on bright supernovae and their hosts from the ASAS-SN team.

Key words: catalogues – surveys – supernovae: general.

1 INTRODUCTION

In recent decades, systematic searches for supernovae have progressed into the era of large projects that survey some or all of the sky for supernovae and other transient phenomena using varying degrees of automation. These projects include the Lick Observatory Supernova Search (LOSS; Li et al. 2000), the Panoramic Survey Telescope and Rapid Response System (Pan-STARRRS; Chambers et al. 2016), the Texas Supernova Search (Quimby 2006), the Sloan Digital Sky Survey (SDSS) Supernova Survey (Frieman et al. 2008), the Catalina Real-Time Transient Survey (CRTS; Drake et al. 2009), the CHilean Automatic Supernova sEarch (Pignata et al. 2009), the Palomar Transient Factory (PTF; Law et al. 2009), the *Gaia* transient survey (Hodgkin et al. 2013), the La Silla-QUEST (LSQ) Low Redshift Supernova Survey (Baltay et al. 2013), the Mobile Astronomical System of TElescope Robots (MASTER; Gorbovskoy et al. 2013) survey, the Optical Gravitational Lensing Experiment-IV (Wyrzykowski et al. 2014) and, recently, the Asteroid Terrestrial-impact Last Alert System (Tonry 2011), among numerous others.

Prior to 2013, however, there was no rapid-cadence optical survey that surveyed the entire visible night sky to find the bright, nearby supernovae that can be studied most comprehensively, and thus have the largest impact on our understanding of supernova physics. This changed with the creation of the All-Sky Automated Survey for SuperNovae (ASAS-SN;[1] Shappee et al. 2014), a long-term project designed to find bright transients, such as nearby supernovae (e.g. Dong et al. 2016; Holoien et al. 2016a; Shappee et al. 2016), tidal disruption events (Holoien et al. 2014a; Brown et al. 2016, 2017; Holoien et al. 2016b,c), flares in active galactic nuclei (Shappee et al. 2014), stellar outbursts (Holoien et al. 2014b; Schmidt et al. 2014; Herczeg et al. 2016; Schmidt et al. 2016) and cataclysmic variable stars (Kato et al. 2014a,b, 2015, 2016).

ASAS-SN accomplishes this using eight telescopes with 14-cm aperture lenses and standard *V*-band filters that have a 4.5 × 4.5 deg.

★ E-mail: tholoien@astronomy.ohio-state.edu (TW-SH); brown@astronomy.ohio-state.edu (JSB); kstanek@astronomy.ohio-state.edu (KZS)
† US Department of Energy Computational Science Graduate Fellow.
‡ Hubble, Carnegie-Princeton Fellow.

[1] http://www.astronomy.ohio-state.edu/assassin/

field of view and a limiting magnitude of $m_V \sim 17$ (see Shappee et al. 2014 for further technical details). The ASAS-SN telescopes are divided into two units, each consisting of four telescopes on a common mount hosted by the Las Cumbres Observatory Global Telescope Network (LCOGT; Brown et al. 2013). Our northern unit, Brutus, is hosted at the LCOGT site on Mount Haleakala in Hawaii, while our southern unit, Cassius, is hosted at the LCOGT site at Cerro Tololo, Chile. These two units give us roughly 20 000 square degrees of coverage per clear night, and we cover the entire observable sky (∼30 000 square degrees on a given night) with a 2–3 d cadence. All data are processed and automatically searched in real-time, which allows for rapid discovery and response, and discoveries are announced publicly, sometimes within a few hours of data collection. For a more detailed history of the ASAS-SN project, see the introduction of Holoien et al. (2017).

Though some professional surveys have more numerous discoveries, all transients discovered by ASAS-SN are bright and relatively nearby, which allows them to be observed over wide wavelength ranges and long time baselines using fairly modest resources. Spectra of ASAS-SN discoveries are often easily obtainable with a 1-m telescope, and all ASAS-SN supernovae have been spectroscopically confirmed and classified. ASAS-SN also uses an untargeted survey approach, which allows us to provide a less biased tool than other surveys for studying the populations of nearby supernovae and their host galaxies.

This manuscript is the second of a series of yearly catalogues provided by the ASAS-SN team and presents the collected information on supernovae discovered by ASAS-SN in 2015 and their host galaxies. As was done in our 2013 and 2014 catalogue (Holoien et al. 2017), we provide the same information for bright supernovae, defined as those with $m_{\rm peak} \leq 17$, discovered by other professional surveys and amateur astronomers in 2015 in order to construct a full sample of bright supernovae discovered in 2015. The analyses and information presented here supersedes our discovery and classification Astronomer's Telegrams (ATels), all of which are cited in this manuscript, and the information publicly available on the ASAS-SN web pages. We also examine simple statistical properties of the combined supernovae sample from this manuscript and from Holoien et al. (2017). Throughout our analyses, we assume a standard Λ cold dark matter cosmology with $H_0 = 69.3\,{\rm km\,s^{-1}\,Mpc^{-1}}$, $\Omega_M = 0.29$ and $\Omega_\Lambda = 0.71$ for converting host redshifts into distances.

In Section 2, we detail the sources of the information presented in this manuscript. In Section 3, we give statistics on the supernovae and hosts in the full, cumulative sample, provide analyses of the data and discuss the overall trends seen in the sample. Finally, in Section 4, we conclude with remarks about the overall findings and look at how future ASAS-SN catalogues will be an integral tool in nearby supernova rate calculations that will be done by the ASAS-SN team.

2 DATA SAMPLES

Here, we describe the sources of the data collected for our supernova and host galaxy samples, which are presented in Tables 1–4.

2.1 The ASAS-SN supernova sample

The ASAS-SN supernova sample is listed in Table 1 and includes all supernovae discovered by ASAS-SN between 2015 January 1 and 2015 December 31. As in Holoien et al. (2017), we collected the names, discovery dates, host names and host offsets for ASAS-SN discoveries from our discovery ATels, which are cited in Table 1. International Astronomical Union (IAU) names are also listed for those supernovae that had one assigned. As we note in our ATels, we view the ASAS-SN names as having priority due to the failure of the IAU system to provide proper credit to the discovery team. We use the IAU system only to avoid temporal reporting conflicts, and encourage others to refer to our discoveries by their ASAS-SN designations.

Redshifts have been spectroscopically measured from classification spectra in all cases. For cases where a redshift had been previously measured for a supernova host galaxy and is consistent with the transient redshift, we list the redshift of the host obtained from the NASA/IPAC Extragalactic Database (NED).[2] For cases where the measurements are not consistent or where a host redshift was not available, we typically report the redshifts given in the classification telegrams.

Supernova classifications are taken from classification telegrams, which we have also cited in Table 1. For those supernovae that had best-fitting ages reported in their classifications, we also give the approximate ages at discovery, measured in days relative to peak. Supernovae were typically classified using either the Supernova Identification code (SNID; Blondin & Tonry 2007) or the Generic Classification Tool (GELATO;[3] Harutyunyan et al. 2008), both of which compare the observed input spectra to template spectra in order to estimate the best supernova type and age match.

Two supernovae, ASASSN-15da and ASASSN-15hx, never had a redshift announced publicly, and we report redshift measurements here. Using the classification spectrum taken with the Ohio State Multi-Object Spectrograph (OSMOS; Martini et al. 2011) mounted on the MDM Observatory Hiltner 2.4-m telescope we measured a redshift of 0.048 ± 0.003 for ASASSN-15da using SNID. We measured a redshift of 0.0081 for ASASSN-15hx using the host-galaxy Hα line detected in a nebular spectrum obtained on 2016 March 11 with the Inamori Magellan Areal Camera and Spectrograph (IMACS; Dressler et al. 2011) mounted on the Magellan-Baade 6.5-m telescope at Las Campanas Observatory.

Based on checking archival classification and late-time spectra of the 2015 ASAS-SN supernova discoveries, we also update a number of redshifts and classifications from the values reported in the discovery and classification telegrams. ASASSN-15al, ASASSN-15az, ASASSN-15bm, ASASSN-15bo, ASASSN-15jm, ASASSN-15lo, ASASSN-15mg, ASASSN-15mx, ASASSN-15nx, ASASSN-15ou, ASASSN-15rg, ASASSN-15sh, ASASSN-15um, ASASSN-15uo, ASASSN-15up and ASASSN-15ug have updated redshifts that have been re-measured from supernova or host spectra obtained with OSMOS on the MDM 2.4-m telescope, IMACS on the Magellan-Baade 6.5-m telescope, the FAst Spectrograph for the Tillinghast Telescope (Fabricant et al. 1998) and the Wide Field Reimaging CCD Camera mounted on the 2.5-m du Pont telescope at Las Campanas Observatory. Based on a re-examination of the classification spectra, we have updated the classifications of ASASSN-15fa, ASASSN-15fr, ASASSN-15fs, ASASSN-15ga, ASASSN-15hy, ASASSN-15jm, ASASSN-15kg, ASASSN-15kj, ASASSN-15mi, ASASSN-15og, ASASSN-15ou, ASASSN-15tg, ASASSN-15um, ASASSN-15uo, ASASSN-15us and ASASSN-15ut. We also report an updated redshift for ASASSN-15ed from Pastorello et al. (2015) and an updated redshift and classification of ASASSN-15no from Benetti et al. (in preparation). These redshifts and classifications are reported in Table 1.

[2] https://ned.ipac.caltech.edu/
[3] gelato.tng.iac.es

Table 1. ASAS-SN supernovae.

SN name	IAU name[a]	Discovery date	RA[b]	Dec.[b]	Redshift	V_{disc}[c]	V_{peak}[c]	Offset (arcsec)[d]	Type	Age at disc.[e]	Host name	Discovery ATel	Classification ATel
ASASSN-15ab	–	2015-01-02.33	210:46:35.04	−38:28:24.6	0.01780	16.3	15.5	25.86	IIn	–	ESO 325-G045	Dong et al. (2015a)	Shappee et al. (2015b)
ASASSN-15ad	–	2014-12-29.18	95:56:13.06	−16:05:51.0	0.02400	16.3	16.3	14.67	Ia	−4	PGC 902451	Shappee et al. (2015a)	Shappee et al. (2015b)
ASASSN-15ae	–	2015-01-01.63	237:46:27.12	+34:25:55.8	0.03124	17.4	16.4	4.98	Ia	−5	2MASX J15510599+3425520	Kiyota et al. (2015a)	Tomasella et al. (2015)
ASASSN-15aj	–	2015-01-08.30	163:13:18.91	−32:55:34.9	0.01092	15.0	14.7	6.36	Ia	−3	NGC 3449	Dong et al. (2015b)	Simon, Morrell & Phillips (2015)
ASASSN-15ak	–	2015-01-09.22	3:00:23.18	+26:23:37.3	0.01503	15.1	14.7	3.36	Ia-91T	–	UGC 00110	Dong et al. (2015c)	Tomasella et al. (2015)
ASASSN-15al	–	2015-01-10.33	74:27:24.44	−21:35:34.1	0.03200	17.0	16.8	7.20	Ia	0	GALEXASC J045749.46	Holoien et al. (2015a)	Fremling et al. (2015a)
ASASSN-15ar	–	2015-01-13.28	37:05:05.39	+10:23:03.8	0.02882	17.6	16.6	21.06	Ia	−6	CGCG 439−010	Kiyota et al. (2015b)	Ochner et al. (2015)
ASASSN-15as	–	2015-01-13.44	144:49:08.26	+6:25:48.5	0.02800	16.4	16.1	3.40	Ia	−1	SDSS J093916.69+062551.1	Gonzalez et al. (2015)	Morrell et al. (2015a)
ASASSN-15az	–	2015-01-14.46	167:09:23.98	−10:14:57.8	0.02832	16.3	16.3	19.00	Ia	−1	2MASX J11083863−1014456	Brimacombe et al. (2015a)	Ochner et al. (2015)
ASASSN-15ba	–	2015-01-15.64	211:13:46.34	+8:55:14.5	0.02313	16.6	15.8	0.86	Ia	−5	SDSS J140455.12+085514.0	Conseil et al. (2015)	Challis, Kirshner & Falco (2015a)
ASASSN-15bb	–	2015-01-16.27	195:16:35.69	−36:36:00.2	0.01587	16.3	16.3	10.24	II	−2	ESO 381-IG048	Kiyota et al. (2015c)	Milisavljevic et al. (2015)
ASASSN-15bc	–	2015-01-16.31	61:33:39.60	−8:53:08.3	0.03672	17.1	16.9	3.64	Ia	−7	2MASX J04061478−0853112	Brimacombe et al. (2015b)	Zhang & Wang (2015a)
ASASSN-15bd	–	2015-01-17.63	238:39:34.96	+16:36:38.1	0.00795	16.8	16.0	1.08	IIb	–	SDSS J155438.39+163637.6	Kiyota et al. (2015d)	Challis et al. (2015b)
ASASSN-15be	–	2015-01-19.07	43:11:35.84	−34:18:52.5	0.02190	16.4	15.6	7.00	Ia	−10	GALEXASC J025245.83	Brimacombe et al. (2015c)	Morrell et al. (2015b)
ASASSN-15bf	–	2015-01-19.12	69:40:16.50	−41:37:26.2	0.04853	17.7	16.1	4.77	Ia	8	2MASX J04384102−4137212	Brimacombe et al. (2015d)	Fremling et al. (2015b)
ASASSN-15bk	–	2015-01-19.62	236:03:06.44	+11:16:16.4	0.03428	17.2	17.1	6.99	Ia	−1	CGCG 078−056	Kiyota et al. (2015e)	Morrell et al. (2015b)
ASASSN-15bm	–	2015-01-22.36	226:27:53.71	−5:37:37.1	0.02060	16.6	15.5	0.14	Ia	−10	GALEXASC J150551.56	Fernandez et al. (2015a)	Morrell et al. (2015b)
ASASSN-15bn	–	2015-01-23.63	238:53:50.24	+66:43:19.3	0.02800	16.7	16.1	7.69	Ia	−2	GALEXASC J155536.57	Brimacombe et al. (2015e)	Zhang & Wang (2015b)
ASASSN-15bo	–	2015-01-22.58	221:13:48.29	+24:34:43.7	0.03630	17.1	16.1	0.32	Ia	−9	SDSS J144455.21+243443.9	Fernandez et al. (2015b)	Benetti et al. (2015)
ASASSN-15cb	–	2015-01-21.54	189:57:33.44	+3:47:49.7	0.04004	16.8	16.8	0.51	Ia	−1	VCC 1810	Holoien et al. (2015b)	Nyholm et al. (2015)

This table is available in its entirety in a machine-readable form in the online journal. A portion is shown here for guidance regarding its form and content. 'GALEXASC' galaxy names have been abbreviated for space reasons.

[a] IAU name is not provided if one was not given to the supernova.

[b] Right ascension and declination are given in the J2000 epoch.

[c] All magnitudes are *V*-band magnitudes from ASAS-SN.

[d] Offset indicates the offset of the SN in arcseconds from the coordinates of the host nucleus, taken from NED.

[e] Discovery ages are given in days relative to peak. All ages are approximate and are only listed if a clear age was given in the classification telegram.

Table 2. Non-ASAS-SN supernovae.

SN name	IAU name[a]	Discovery date	RA[b]	Dec.[b]	Redshift	m_{peak}[c]	Offset (arcsec)[d]	Type	Host name	Discovered by[e]	Recovered?[f]
2015B	2015B	2015-01-05.12	12:54:35.53	−12:34:18.6	0.01544	15.0	10.20	Ia	NGC 4782	Amateurs	Yes
LSQ15z	–	2015-01-07.00	13:08:22.48	−8:43:57.8	0.07000	17.0	3.06	Ia	2MASX J13082255−0844002	LSQ	No
2015C	2015C	2015-01-07.60	13:18:30.47	−14:36:44.6	0.00964	16.4	12.60	II	IC 4221	LOSS	No
2015A	2015A	2015-01-09.64	9:41:15.55	35:53:17.4	0.02339	16.6	24.70	Ia	NGC 2955	Amateurs	Yes
PSN J13522411+3941286	–	2015-01-09.90	13:52:24.11	39:41:28.6	0.00722	15.6	18.65	IIn	NGC 5337	Amateurs	Yes
2015W	2015W	2015-01-12.28	6:57:43.03	13:34:45.7	0.01329	16.2	34.89	II	UGC 03617	LOSS	Yes
2015E	2015E	2015-01-13.42	3:13:35.31	0:15:03.1	0.04145	16.1	1.61	Ia	KUG 0311+000	KISS	No
CSS150120:053013−165338	–	2015-01-20.00	5:30:13.08	−16:53:37.1	0.02000	17.0	N/A	II	None	CRTS	No
PSN J11105565+5322493	–	2015-01-23.14	11:10:55.65	53:22:49.3	0.00955	17.0	29.15	II	NGC 3549	CRTS	No
PSN J10491665−1938253	–	2015-02-02.00	10:49:16.65	−19:38:25.3	0.01403	16.8	12.04	IIP	ESO 569-G012	Amateurs	No
2015bh	2015bh	2015-02-07.39	9:09:34.96	33:07:20.4	0.00649	15.4	16.40	IIn/LBV	NGC 2770	CRTS	Yes
2015H	2015H	2015-02-10.54	10:54:42.16	−21:04:13.8	0.01246	16.0	33.11	Ia-02cx	NGC 3464	Amateurs	Yes
PSN J13471211−2422171	–	2015-02-12.52	13:47:12.11	−24:22:17.1	0.01991	15.1	6.08	Ia	ESO 509-G108	Amateurs	Yes
PSN J10234760+3348477	–	2015-02-13.31	10:23:47.60	33:48:47.7	0.03389	17.0	23.02	IIb	UGC 05623	Amateurs	No
2015U	2015U	2015-02-13.34	7:28:53.87	33:49:10.6	0.01379	14.9	5.92	Ibn	NGC 2388	LOSS	Yes
iPTF15ku	2015bq	2015-02-14.43	12:35:06.37	31:14:35.4	0.02818	16.9	15.00	Ia-91T	KUG 1232+315	PTF	Yes
CSS150214:140955+173155	2015bo	2015-02-14.44	14:09:55.13	17:31:55.6	0.01620	16.8	59.08	Ia-91bg	NGC 5490	CRTS	Yes
PSN J19235601−5955321	–	2015-02-16.64	19:23:56.01	−59:55:32.1	0.01308	15.1	18.60	Ia	NGC 6782	Amateurs	No
PSN J20580766−5147074	–	2015-02-22.13	20:58:07.66	−51:47:07.4	0.01567	16.3	10.20	IIb	FAIRALL 0927	Amateurs	No
2015X	2015X	2015-02-23.22	7:16:42.58	29:51:22.7	0.01072	16.0	6.24	II	UGC 03777	LOSS	No

This table is available in its entirety in a machine-readable form in the online journal. A portion is shown here for guidance regarding its form and content.

[a] IAU name is not provided if one was not given to the supernova. In some cases the IAU name may also be the primary supernova name.

[b] Right ascension and declination are given in the J2000 epoch.

[c] All magnitudes are taken from D. W. Bishop's Bright Supernova website, as described in the text, and may be from different filters.

[d] Offset indicates the offset of the SN in arcseconds from the coordinates of the host nucleus, taken from NED.

[e] 'Amateurs' indicates discovery by any number of non-professional astronomers, as described in the text.

[f] Indicates whether the supernova was independently recovered in ASAS-SN data or not.

Table 3. ASAS-SN supernova host galaxies.

Galaxy name	Redshift	SN name	SN type	SN offset (arcsec)	A_V[a]	m_{NUV}[b]	m_u[c]	m_g[c]	m_r[c]	m_i[c]	m_z[c]	m_J[d]	m_H[d]	m_{K_S}[d,e]	m_{W1}	m_{W2}
ESO 325-G045	0.01780	ASASSN-15ab	IIn	27.03	0.301	16.36 0.02	–	–	–	–	–	14.81 0.08	14.10 0.09	13.95 0.16	13.08 0.03	12.97 0.03
PGC 902451	0.02400	ASASSN-15ad	Ia	14.67	0.577	–	–	–	–	–	–	>16.5	>15.7	13.96 0.07*	14.60 0.03	14.64 0.05
2MASX J15510599+3425520	0.03124	ASASSN-15ae	Ia	4.98	0.085	17.62 0.03	17.56 0.02	16.27 0.00	15.83 0.00	15.59 0.00	15.45 0.01	15.02 0.09	14.66 0.16	14.22 0.15	14.26 0.03	14.11 0.04
NGC 3449	0.01092	ASASSN-15aj	Ia	6.36	0.209	16.17 0.03	–	–	–	–	–	9.70 0.02	9.00 0.02	8.70 0.03	9.60 0.02	9.57 0.02
UGC 00110	0.01503	ASASSN-15ak	Ia-91T	3.6	0.118	17.00 0.01	16.66 0.02	15.36 0.00	14.88 0.00	14.67 0.00	14.61 0.01	>16.5	>15.7	13.35 0.07*	13.99 0.03	13.85 0.04
GALEXASC J045749.46	0.03200	ASASSN-15al	Ia	7.2	0.094	18.91 0.07	–	–	–	–	–	>16.5	>15.7	14.71 0.07*	15.35 0.04	15.08 0.06
CGCG 439-010	0.02882	ASASSN-15ar	Ia	21.06	0.299	–	–	–	–	–	–	12.33 0.03	11.66 0.04	11.30 0.07	12.15 0.02	12.11 0.02
SDSS J093916.69+062551.1	0.02800	ASASSN-15as	Ia	3.4	0.124	21.73 0.14	21.02 0.23	19.85 0.04	19.61 0.05	19.44 0.06	19.56 0.22	>16.5	>15.7	>15.6	–	–
2MASX J11083863−1014456	0.02832	ASASSN-15az	Ia	19	0.171	21.80 0.46	–	–	–	–	–	13.76 0.06	13.03 0.05	12.63 0.10	12.98 0.04	13.02 0.04
SDSS J140455.12+085514.0	0.02313	ASASSN-15ba	Ia	0.86	0.070	19.76 0.04	19.19 0.10	18.04 0.02	17.59 0.02	17.36 0.02	17.21 0.06	>16.5	>15.7	15.73 0.08*	16.37 0.06	16.14 0.17
ESO 381-IG048	0.01587	ASASSN-15bb	II	10.24	0.130	16.20 0.02	–	–	–	–	–	>16.5	>15.7	12.54 0.06*	13.18 0.02	12.95 0.03
2MASX J04061478−0853112	0.03672	ASASSN-15bc	Ia	3.64	0.119	–	–	–	–	–	–	14.02 0.06	13.36 0.07	13.05 0.11	13.11 0.03	12.95 0.03
SDSS J155438.39+163637.6	0.00795	ASASSN-15bd	IIb	1.08	0.094	–	17.70 0.02	16.99 0.00	16.65 0.00	16.57 0.01	16.48 0.01	>16.5	>15.7	14.09 0.07*	14.73 0.03	14.60 0.05
GALEXASC J025245.83	0.02190	ASASSN-15be	Ia	7	0.054	18.61 0.05	–	–	–	–	–	>16.5	>15.7	14.95 0.07*	15.59 0.04	15.41 0.07
2MASX J04384102−4137212	0.04853	ASASSN-15bf	Ia	4.77	0.069	–	–	–	–	–	–	13.77 0.06	13.21 0.08	12.99 0.13	12.62 0.09	12.53 0.02
CGCG 078−056	0.03428	ASASSN-15bk	Ia	6.99	0.125	18.23 0.02	17.30 0.02	15.80 0.00	15.02 0.00	14.61 0.00	14.27 0.01	13.45 0.05	12.73 0.05	12.37 0.09	12.54 0.02	12.38 0.02
GALEXASC J150551.56	0.02060	ASASSN-15bm	Ia	0.14	0.221	17.87 0.05	–	–	–	–	–	12.92 0.05	12.35 0.07	11.84 0.09	12.21 0.02	12.20 0.02
GALEXASC J155536.57	0.02800	ASASSN-15bn	Ia	7.69	0.086	18.83 0.06	–	–	–	–	–	>16.5	>15.7	14.61 0.07*	15.25 0.03	15.19 0.05
SDSS J144455.21+243443.9	0.03630	ASASSN-15bo	Ia	0.32	0.116	20.67 0.28	19.73 0.05	18.70 0.01	18.28 0.01	18.05 0.01	17.86 0.03	>16.5	>15.7	15.19 0.07*	15.83 0.04	16.00 0.12
VCC 1810	0.04004	ASASSN-15cb	Ia	0.51	0.090	17.56 0.01	16.79 0.01	15.64 0.00	15.14 0.00	14.86 0.00	14.67 0.01	13.73 0.06	12.96 0.06	12.96 0.12	12.75 0.02	12.56 0.03

This table is available in its entirety in a machine-readable form in the online journal. A portion is shown here for guidance regarding its form and content. Uncertainty is given for all magnitudes, and in some cases is equal to zero. 'GALEXASC' galaxy names have been abbreviated for space reasons.

[a] Galactic extinction taken from Schlafly & Finkbeiner (2011).

[b] No magnitude is listed for those galaxies not detected in *GALEX* survey data.

[c] No magnitude is listed for those galaxies not detected in SDSS data or those located outside of the SDSS footprint.

[d] For those galaxies not detected in 2MASS data, we assume an upper limit of the faintest galaxy detected in each band from our sample.

[e] K_S-band magnitudes marked with a '*' indicate those estimated from the *WISE* $W1$-band data, as described in the text.

Table 4. Non-ASAS-SN supernova host galaxies.

Galaxy name	Redshift	SN name	SN type	SN offset (arcsec)	A_V[a]	m_{NUV}[b]	m_u[c]	m_g[c]	m_r[c]	m_i[c]	m_z[c]	m_J[d]	m_H[d]	m_{K_S}[d,e]	m_{W1}	m_{W2}
NGC 4782	0.01544	2015B	Ia	10.20	0.146	16.65 0.01	–	–	–	–	–	8.82 0.01	8.10 0.01	7.83 0.02	9.48 0.02	9.54 0.02
2MASX J13082255−0844002	0.07000	LSQ15z	Ia	3.06	0.098	19.57 0.07	–	–	–	–	–	15.05 0.09	14.32 0.10	13.93 0.15	13.54 0.03	13.16 0.03
IC 4221	0.00964	2015C	II	12.60	0.223	–	–	–	–	–	–	11.41 0.03	10.72 0.03	10.48 0.06	11.65 0.02	11.61 0.02
NGC 2955	0.02339	2015A	Ia	24.70	0.030	15.71 0.02	14.69 0.00	13.22 0.00	12.60 0.00	12.19 0.00	11.89 0.00	11.16 0.02	10.47 0.04	10.17 0.03	10.67 0.02	10.52 0.02
NGC 5337	0.00722	PSN J13522411	IIn	18.65	0.039	16.47 0.01	14.82 0.01	13.21 0.00	12.49 0.00	12.12 0.00	11.81 0.00	10.97 0.02	10.32 0.02	10.07 0.03	11.13 0.02	11.19 0.02
UGC 03617	0.01329	2015W	II	34.89	0.380	–	–	–	–	–	–	14.18 0.05	13.56 0.07	13.48 0.10	13.69 0.03	13.58 0.03
KUG 0311+000	0.04145	2015E	Ia	1.61	0.229	19.28 0.02	18.21 0.02	16.82 0.00	16.15 0.00	15.77 0.00	15.47 0.01	14.29 0.04	13.59 0.05	13.40 0.07	13.07 0.03	12.93 0.03
None	0.02000	CSS150120:053013	II	N/A	0.193	–	–	–	–	–	–	>16.5	>15.7	15.94 0.15*	16.58 0.14	16.70 0.35
NGC 3549	0.00955	PSN J11105565	II	29.15	0.035	15.19 0.00	14.61 0.01	12.82 0.00	12.04 0.00	11.67 0.00	11.41 0.00	10.15 0.02	9.45 0.02	9.18 0.03	11.45 0.03	11.51 0.02
ESO 569-G012	0.01403	PSN J10491665	IIP	12.04	0.111	16.79 0.02	–	–	–	–	–	10.67 0.02	9.93 0.02	9.61 0.03	9.85 0.02	9.69 0.02
NGC 2770	0.00649	2015bh	IIn/LBV	16.40	0.062	14.79 0.01	–	–	–	–	–	10.52 0.02	9.81 0.03	9.57 0.04	11.64 0.02	11.59 0.02
NGC 3464	0.01246	2015H	Ia-02cx	33.11	0.150	14.99 0.01	15.22 0.01	13.45 0.00	12.61 0.00	12.18 0.00	11.87 0.00	10.61 0.03	9.89 0.03	9.65 0.05	11.27 0.02	11.27 0.02
ESO 509-G108	0.01991	PSN J13471211	Ia	6.08	0.203	19.17 0.10	–	–	–	–	–	10.99 0.02	10.29 0.03	10.03 0.03	10.44 0.02	10.53 0.02
UGC 05623	0.03389	PSN J10234760	IIb	23.02	0.067	–	16.88 0.02	15.78 0.00	15.37 0.00	15.18 0.00	15.02 0.01	>16.5	>15.7	13.76 0.07*	14.40 0.03	14.09 0.04
NGC 2388	0.01379	2015U	Ibn	5.92	0.159	18.00 0.03	16.21 0.01	14.28 0.00	13.12 0.00	12.56 0.00	12.05 0.00	10.83 0.01	10.03 0.02	9.65 0.02	9.63 0.02	9.16 0.02
KUG 1232+315	0.02818	iPTF15ku	Ia-91T	15.00	0.037	18.45 0.00	18.11 0.03	17.01 0.01	16.55 0.01	16.31 0.01	16.12 0.02	>16.5	>15.7	14.33 0.07*	14.97 0.03	14.72 0.06
NGC 5490	0.01620	CSS150214:140955	Ia-91bg	59.08	0.073	17.92 0.04	14.77 0.01	12.75 0.00	11.91 0.00	11.49 0.00	11.21 0.00	10.01 0.01	9.30 0.02	9.03 0.02	9.71 0.02	9.75 0.02
NGC 6782	0.01308	PSN J19235601	Ia	18.60	0.163	15.48 0.00	–	–	–	–	–	9.90 0.01	9.21 0.02	8.96 0.02	9.62 0.02	9.54 0.02
FAIRALL 0927	0.01567	PSN J20580766	IIb	10.20	0.099	–	–	–	–	–	–	11.86 0.03	11.12 0.04	10.86 0.05	11.08 0.02	10.85 0.02
UGC 03777	0.01072	2015X	II	6.24	0.162	–	21.74 0.17	20.75 0.07	19.36 0.02	19.05 0.02	18.76 0.05	12.03 0.04	11.33 0.05	11.04 0.07	11.93 0.02	11.86 0.02

This table is available in its entirety in a machine-readable form in the online journal. A portion is shown here for guidance regarding its form and content. Uncertainty is given for all magnitudes, and in some cases is equal to zero. 'PSN' and 'CSS' supernova names have been abbreviated for space reasons.

[a] Galactic extinction taken from Schlafly & Finkbeiner (2011).

[b] No magnitude is listed for those galaxies not detected in *GALEX* survey data.

[c] No magnitude is listed for those galaxies not detected in SDSS data or those located outside of the SDSS footprint.

[d] For those galaxies not detected in 2MASS data, we assume an upper limit of the faintest galaxy detected in each band from our sample.

[e] K_S-band magnitudes marked with a '*' indicate those estimated from the *WISE W*1-band data, as described in the text.

For all ASAS-SN supernovae we solved the astrometry in follow-up images using astrometry.net (Barron et al. 2008) and measured a centroid position for the supernova using IRAF, which typically yielded errors of <1.0 arcsec in position. This is significantly more accurate than measuring the coordinates directly from ASAS-SN images, which have a 7.0 arcsec pixel scale. Follow-up images used to measure astrometry were obtained using the LCOGT 1-m telescopes at McDonald Observatory, Cerro Tololo Inter-American Observatory, Siding Springs Observatory and the South African Astronomical Observatory (Brown et al. 2013); OSMOS mounted on the MDM Hiltner 2.4-m telescope; the Las Campanas Observatory Swope 1-m telescope; IMACS mounted on the Magellan-Baade 6.5-m telescope; or from amateur collaborators working with the ASAS-SN team. In most cases, we reported coordinates measured from follow-up images in our discovery telegrams, but we report new, more accurate coordinates in Table 1 for supernovae that were announced with coordinates measured from ASAS-SN data.

We have re-measured *V* band, host-subtracted discovery and peak magnitudes from ASAS-SN data for all ASAS-SN supernova discoveries and report these magnitudes in Table 1. In some cases, re-reductions of the ASAS-SN data have resulted in differences between the magnitudes given in Table 1 and those in the original discovery ATels. Here, the 'discovery magnitude' is defined as the magnitude on the announced discovery date. We also performed a parabolic fit to the measured magnitudes for cases with enough detections, and we use the brighter value between the peak of the fit and the brightest measured magnitude as the 'peak magnitude' reported in Table 1. For cases with too few detections for a parabolic fit, we use the brightest measured magnitude as the peak magnitude.

One supernova, ASASSN-15kn, was announced by ASAS-SN in an ATel and was later announced by the Italian Supernovae Search Project (ISSP)[4] in the Central Bureau for Astronomical Telegram with the name PSNJ12415045−0710122. The ISSP discovery image was obtained prior to the ASAS-SN discovery image, but since we announced it first, we list it as an ASAS-SN discovery with its ASAS-SN name in Table 1.

All supernovae discovered by ASAS-SN in 2015 are included in this catalogue, including those that were fainter than $m_V = 17$, but in the comparison analyses presented in Section 3 we exclude those supernovae with $m_{V,\,\mathrm{peak}} > 17$ so that our sample matches the non-ASAS-SN sample.

2.2 The non-ASAS-SN supernova sample

Table 2 gives information for the sample of bright supernovae that were not discovered by ASAS-SN. This sample includes all spectroscopically confirmed supernovae with peak magnitudes $m_{\mathrm{peak}} \leq 17$ discovered between 2015 January 1 and 2015 December 31.

Data for these non-ASAS-SN discoveries were compiled from the 'latest supernovae' website[5] maintained by D. W. Bishop (Gal-Yam et al. 2013). This page provides a repository of discoveries reported from different channels and attempts to link objects reported by different sources at different times, and thus provides the best available source in 2015 for collecting information on supernovae discovered by different sources. The names, IAU names, discovery dates, coordinates, host names, host offsets, peak magnitudes, types and discovery sources that are listed in Table 2 were taken from this page when possible. Redshifts for host galaxies were retrieved from NED when available, and were taken from the latest supernovae website when previous host measurements were not available. For cases where the website did not list a host name or host offset for the supernova, this information was taken from NED. We define the offset in these cases as the difference between the reported supernova coordinates and the galaxy coordinates in NED. For all supernovae in both samples, we give the primary name of the host galaxy from NED, which sometimes differs from the name listed on the ASAS-SN supernova page or the latest supernovae website.

We list the name of the discovery group for all supernovae discovered by other professional surveys. For supernovae discovered by non-professional astronomers, we list a discovery source of 'Amateurs' in order to distinguish these supernovae from those discovered by ASAS-SN and other professional surveys. As was the case in 2014, amateurs accounted for the largest number of bright supernova discoveries after ASAS-SN in 2015.

Lastly, we note in Table 2 whether these supernovae were independently recovered while scanning ASAS-SN data so that we can quantify the impact ASAS-SN would have on the discovery of bright supernovae without the presence of other supernova searches. In Section 3.2, we examine the cases of the two very bright ($m_{\mathrm{peak}} < 15$) supernovae from 2015 that were not recovered by ASAS-SN in order to determine why ASAS-SN missed these supernovae despite its large coverage area and high cadence.

2.3 The host galaxy samples

We have collected Galactic extinction values and magnitudes in various photometric filters spanning from the near-ultraviolet (NUV) to the infrared (IR) for all host galaxies of the supernovae in both the ASAS-SN and the non-ASAS-SN samples. These data are presented in Tables 3 and 4 for ASAS-SN hosts and non-ASAS-SN hosts, respectively. The Galactic A_V is taken from Schlafly & Finkbeiner (2011) and was gathered from NED for the supernova position. We obtained NUV magnitudes from the *Galaxy Evolution Explorer* (*GALEX*) All Sky Imaging Survey (AIS), optical *ugriz* magnitudes from the SDSS Data Release 12 (SDSS DR12; Alam et al. 2015), IR JHK_S magnitudes from the Two-Micron All Sky Survey (2MASS; Skrutskie et al. 2006), and *W*1 and *W*2 magnitudes from the *Wide-field Infrared Survey Explorer* (*WISE*; Wright et al. 2010) AllWISE source catalogue. For cases where the host is not detected in 2MASS data, we adopt an upper limit that corresponds to the faintest detected host magnitude in our sample ($m_J > 16.5$, $m_H > 15.7$) for the *J* and *H* bands.

For the K_S band, we estimate a host magnitude for those hosts that are not detected in 2MASS but are detected in the *WISE W*1-band by adding the mean $K_S - W1$ offset from the sample to the *WISE W*1 data. We calculated this offset by averaging the offsets for all hosts that were detected in both the K_S and *W*1 bands from both supernova samples, and it is equal to −0.64 magnitudes with a scatter of 0.05 magnitudes and a standard error of 0.002 magnitudes. This agrees well with the offset calculated with the 2014 sample in Holoien et al. (2017). For hosts that are not detected in either 2MASS or *WISE*, we again adopt an upper limit corresponding to the faintest detected host in that filter, $m_{K_S} > 15.6$.

3 ANALYSIS

Here, we provide some basic statistical analyses of the supernova samples and examine reasons why ASAS-SN does not recover some very bright supernovae.

[4] http://italiansupernovae.org/
[5] http://www.rochesterastronomy.org/snimages/

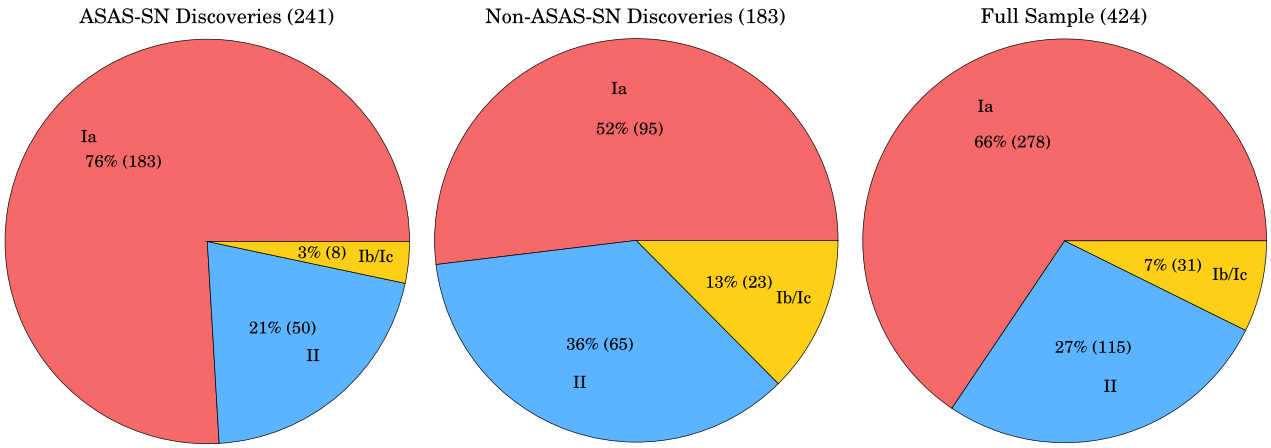

Figure 1. Left-hand panel: Pie chart breaking down the ASAS-SN sample of supernovae discovered between 2014 May 1 and 2015 December 31 by type. The fractional breakdown is quite similar to that of an ideal magnitude-limited sample from Li et al. (2011). Center panel: the same breakdown of supernova types for the non-ASAS-SN sample from the same time period. Right-hand panel: the same breakdown of supernova types for the combined sample. Type IIb supernovae are considered part of the 'Type II' sample for this analysis.

3.1 Sample analyses

Combining all the bright supernovae from both samples discovered between 2014 May 1, when ASAS-SN became operational in both hemispheres and 2015 December 31 provides a total sample of 425 supernovae, after excluding those ASAS-SN discoveries with $m_{\rm peak} > 17.0$. Of these, 57 per cent (242) were discovered by ASAS-SN, 25 per cent (105) were discovered by amateurs and 18 per cent (78) were discovered by other professional surveys. By type, 278 were Type Ia supernovae, 115 were Type II supernovae and 31 were Type Ib/Ic supernovae. Following Li et al. (2011), we include Type IIb supernovae in the Type II sample to allow a more direct comparison with their results. ASASSN-15lh is either a Type I superluminous supernova (SLSN-I; Dong et al. 2016; Godoy-Rivera et al. 2017) or a tidal disruption event around a Kerr black hole (Leloudas et al. 2016), and we do not include it in analyses that look at trends by type. ASAS-SN discovered 66 per cent (183) of the Type Ia supernovae, 43 per cent (50) of the Type II supernovae and 26 per cent (8) of the Type Ib/Ic supernovae. Amateurs discovered 20 per cent (55), 31 per cent (36) and 48 per cent (15) of the Type Ia, Type II and Type Ib/Ic supernovae, respectively, while other professional surveys accounted for the remaining 15 per cent (41), 25 per cent (29) and 26 per cent (8) of each.

In Fig. 1, we show a breakdown by type of the supernovae in the ASAS-SN sample, the non-ASAS-SN sample and the combined sample. As would be expected from a magnitude-limited sample, Type Ia supernovae represent the largest fraction of supernovae in all three samples (e.g. Li et al. 2011). The ASAS-SN sample has the highest fraction of Type Ia supernovae of the three samples, and matches the 'ideal magnitude-limited sample' breakdown (79 per cent Type Ia, 17 per cent Type II and 4 per cent Type Ib/Ic) predicted from the LOSS volume-limited sample in Li et al. (2011) almost exactly. As was the case with just the 2014 sample, the non-ASAS-SN sample and the overall sample have higher fractions of Type II and Type Ib/Ic supernovae (Holoien et al. 2017).

Although ASAS-SN discovers fewer supernovae overall than other professional surveys, ASAS-SN has been the dominant source of bright supernova discoveries since becoming operational in both hemispheres in May of 2014. Trends seen in the 2014 sample (Holoien et al. 2017) continue in the 2015 sample as well. ASAS-SN often discovers supernovae shortly after explosion due to its rapid cadence: 217 of the ASAS-SN supernovae have approximate measured ages at discovery and 70 per cent (151) were discovered prior to reaching their peak brightness.

ASAS-SN also continues to be less affected by host galaxy selection effects than other bright supernova searches: 24 per cent (57) of the ASAS-SN bright supernovae were discovered in catalogued host galaxies without known redshifts, while only 14 per cent (26) of the supernovae discovered by other sources were found in such hosts. An additional 3 per cent (7) of the ASAS-SN supernovae were found in uncatalogued hosts or have no apparent host galaxy compared to 1 per cent (2) of the non-ASAS-SN discoveries, indicating that ASAS-SN is less biased against finding supernovae in uncatalogued hosts.

ASAS-SN discoveries continue to stand out from bright supernovae discovered by other sources with regards to their offsets from their host galaxy nuclei. In Fig. 2, we show the host K_S-band absolute magnitude and the offset from host nucleus for all supernovae in our sample, with the median values for each source (ASAS-SN, amateurs or other professionals) marked with horizontal and vertical lines. To help put the overall magnitude scale in perspective, a typical $L_\star$ galaxy has $M_{\star,K_S} = -24.2$ (Kochanek et al. 2001), and a corresponding luminosity scale is given on the upper axis of the figure.

Amateur surveys are significantly biased towards luminous galaxies and larger offsets from the host nucleus, which is unsurprising given that they tend to observe bright, nearby galaxies and use less sophisticated detection techniques than professional surveys. This approach allows amateur observers to obtain many observations of such galaxies per night, increasing their chances of finding supernovae, but it biases them against finding supernovae in fainter hosts. Other professional surveys in our comparison sample do discover supernovae with smaller angular separations than amateurs (median value of 12.2 arcsec versus 15.0 arcsec), but in terms of physical separation both samples exhibit a similar median offset (4.8 kpc for professionals, 5.1 kpc for amateurs). Conversely, ASAS-SN discoveries have median offsets of 4.9 arcsec and 2.6 kpc, indicating that ASAS-SN is less biased against discoveries close to the host nucleus than either comparison group. The three other professional groups with the most discoveries in our comparison sample are

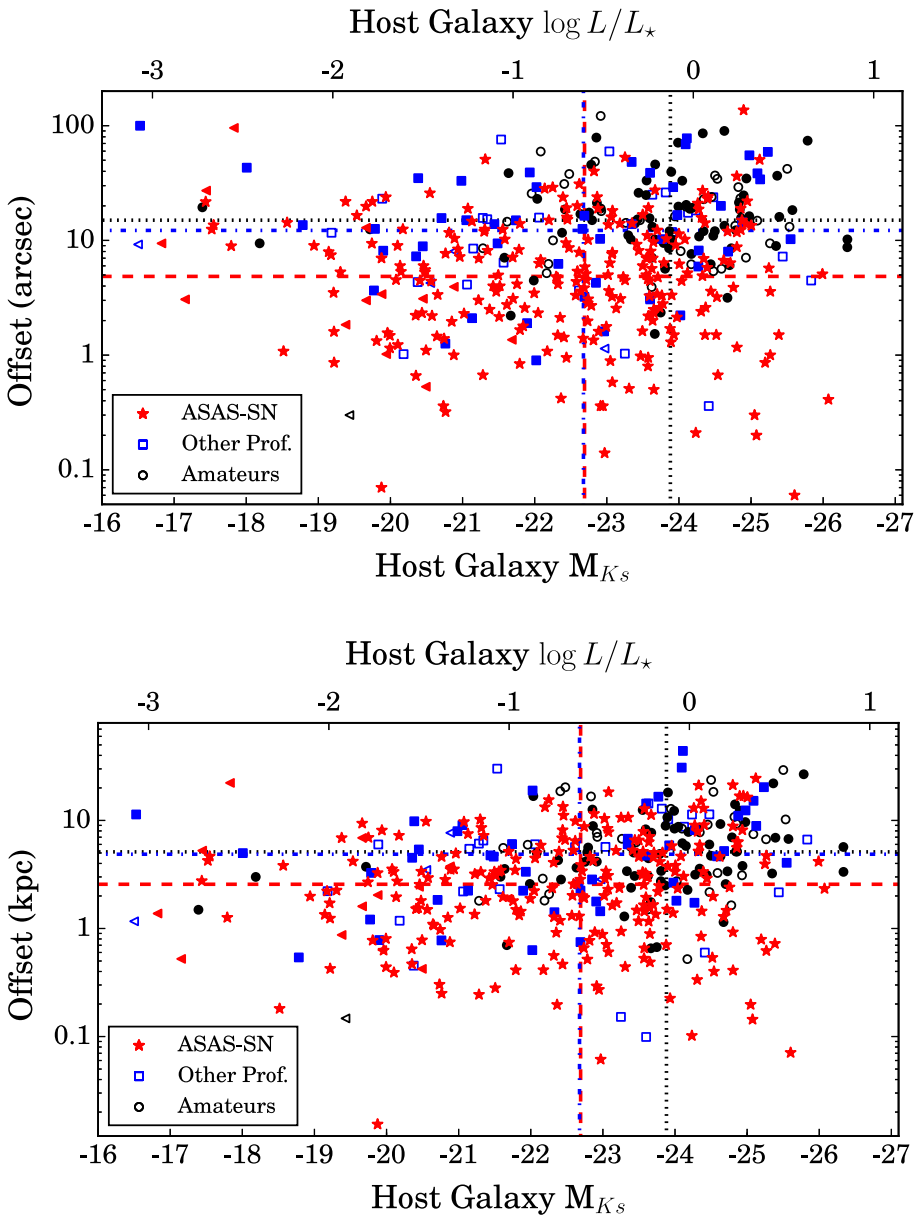

Figure 2. *Upper panel*: absolute K_S-band host galaxy magnitude versus the offset from host nucleus in arcseconds for our total bright supernova sample. The upper axis gives the log $(L/L_\star)$ values corresponding to the magnitude scale for $M_{\star,K_S} = -24.2$ (Kochanek et al. 2001). Supernovae discovered by ASAS-SN are shown as red stars, those discovered by amateur observers are shown as black circles, and those discovered by other professional surveys are shown as blue squares. Filled points indicate supernovae that were independently recovered by ASAS-SN. Triangles are used to indicate upper limits on host galaxy magnitudes for hosts that were not detected by either 2MASS or *WISE*. Median offsets and magnitudes for ASAS-SN, Amateurs and other professionals are indicated by dashed, dotted and dash–dotted lines, respectively, in colours matching the data points. Upper limits are included in computing the median magnitudes. *Lower panel*: as above, but with the offset measured in kiloparsecs rather than arcseconds.

CRTS (Drake et al. 2009), MASTER (Gorbovskoy et al. 2013) and LOSS (Li et al. 2000), which either do not use difference imaging or ignore central regions of galaxies in their searches, and this likely contributes to their larger offsets. As we pointed out in Holoien et al. (2017), however, ASAS-SN continues to find a higher rate of tidal disruption events than other surveys (see Holoien et al. 2016c,b), including those that do use difference imaging, which implies that the avoidance of the central regions of galaxies is still fairly common in surveys other than CRTS, MASTER and LOSS.

The median host magnitudes for supernovae discovered by ASAS-SN, other professionals and amateurs are $M_{K_S} \simeq -22.7$, $M_{K_S} \simeq -22.7$ and $M_{K_S} \simeq -23.8$, respectively. While the median host magnitude for other professionals' discoveries is slightly fainter than that for ASAS-SN discoveries, the measurements are consistent given the uncertainties. There is however a clear distinction between professional surveys (including ASAS-SN) and amateurs.

ASAS-SN has had a significant impact on the discovery of bright supernovae. One way this can be seen is by looking at the number of bright supernovae discovered per month in 2013, 2014 and 2015. Fig. 3 shows a histogram of supernovae with $m_{\rm peak} \leq 17$ discovered by ASAS-SN and those discovered by other sources in each month of 2013, 2014 and 2015. As was the case in Holoien et al. (2017), we include information for all bright supernovae discovered in the early months of 2014 for completeness, and we add the same information

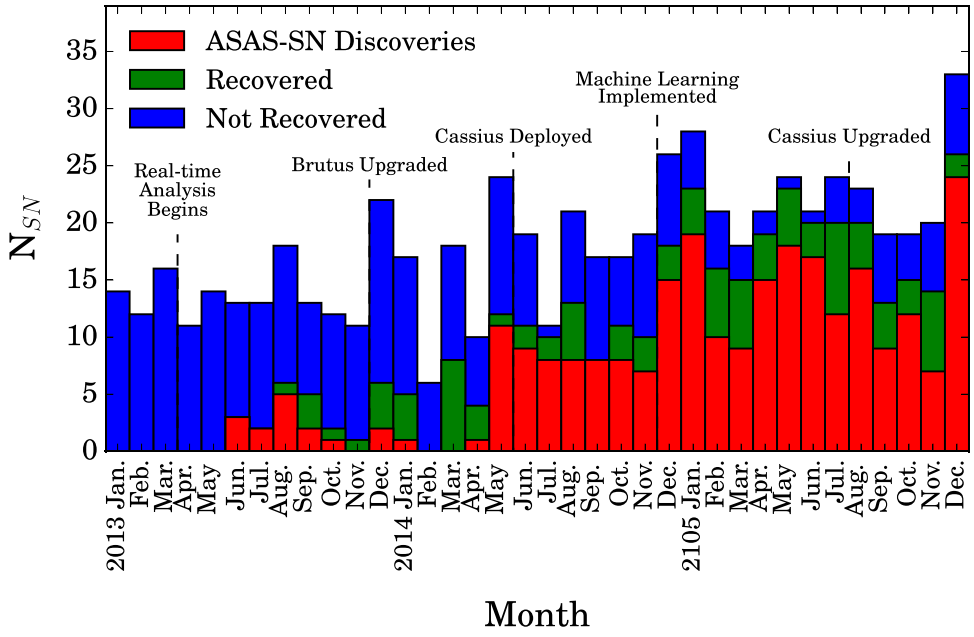

Figure 3. Histogram of bright supernovae discoveries in each month of 2013, 2014 and 2015. ASAS-SN discoveries are indicated in red, supernovae discovered by other sources and independently recovered by ASAS-SN are indicated in green, and supernovae that were not recovered by ASAS-SN are indicated in blue. Significant milestones in the ASAS-SN timeline are also indicated. The impact of ASAS-SN becoming operational in both hemispheres in 2014 May is clearly seen by a large increase in discoveries in all following months. ASAS-SN accounts for at least half of the bright supernova discoveries in every month after 2014 April, and also recovers a significant fraction of the supernovae it does not discover, particularly in 2015.

for all of 2013 as well to expand our comparison. To help show the impact of various improvements to the ASAS-SN hardware and software, we indicate certain milestones, such as the deployment of our southern unit Cassius and its upgrade to four telescopes, on the figure as well.

Before our southern unit Cassius became operational, other supernova searches were discovering the majority of bright, nearby supernovae. However, as can be seen in Fig. 3, the addition of Cassius and improvements to our pipeline had a major impact on our detection efficiency. For every month of 2014 and 2015 after the deployment of Cassius, ASAS-SN discovers or independently recovers at least half of all bright supernovae, and often this fraction is significantly larger. The average number of bright supernovae discovered per month has also increased substantially since ASAS-SN became operational in both hemispheres, from 14 with a scatter of 4 supernovae per month to 21 with a scatter of 5 supernovae per month. This implies that the rate of bright supernovae discovered per month has increased from $\sim 13 \pm 2$ supernovae per month prior to Cassius becoming operational to $\sim 21 \pm 2$ supernovae per month afterwards, providing roughly 4σ evidence that the discovery rate has increased since Cassius was deployed. This suggests that ASAS-SN is discovering supernovae that would not otherwise be discovered by other supernova searches, and thus that we can now construct a more complete sample of bright, nearby supernovae.

ASAS-SN is also less biased in terms of the locations of its discoveries. Fig. 4 shows a cumulative normalized histogram of supernovae with respect to the sine of their declination. The green dashed line represents what would be expected if supernovae were discovered at all declinations equally. As can be seen in the figure, supernovae discovered by non-ASAS-SN sources have a clear bias towards the Northern hemisphere: the non-ASAS-SN histogram falls significantly below the 'no bias' expectation except at very low [$\sin(\mathrm{Dec}) \lesssim -0.8$] and very high [$\sin(\mathrm{Dec}) \gtrsim 0.6$] declinations.

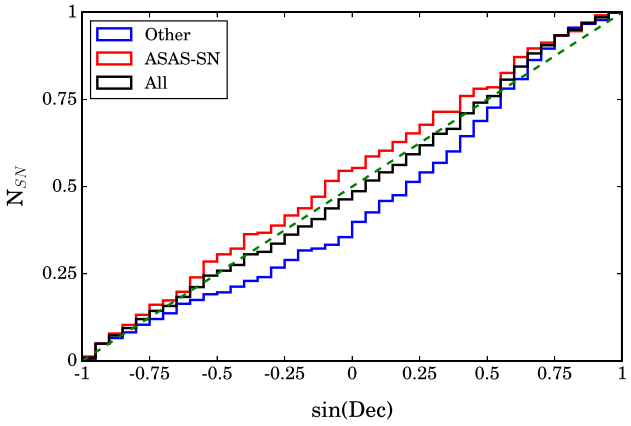

Figure 4. Cumulative normalized histogram of supernova discoveries with respect to the sine of their declination. ASAS-SN discoveries are shown in red, non-ASAS-SN discoveries are shown in blue and the combined sample is shown in black. The green dashed line represents what would be expected if supernovae were equally likely to be discovered at all declinations. Non-ASAS-SN discoveries have a clear northern bias and fall well below the expectation except near the poles, while ASAS-SN discoveries correct this trend.

This is not unexpected, as many professional searches are based in the Northern hemisphere. The ASAS-SN discoveries make the combined sample (the black line) follow the expected distribution very closely. The primary bias remaining in sky coverage is the Galactic plane.

The redshift distribution of our full sample, divided by supernova type, is shown in Fig. 5. There is a clear distinction between the redshifts of Type Ia and Type II supernovae in our sample, with the Type II distribution peaking at $z \lesssim 0.01$ and the Type Ia distribution

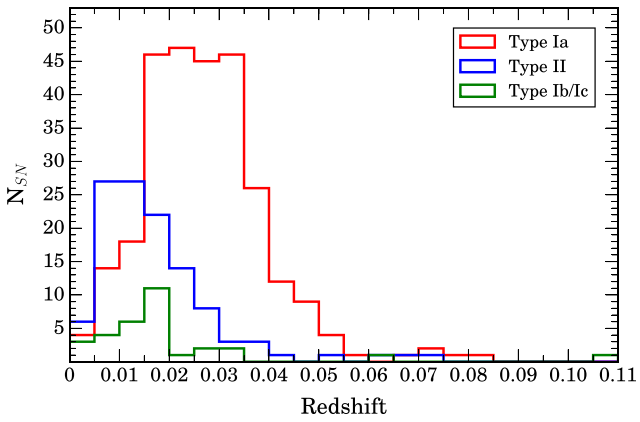

Figure 5. Histograms of the supernova redshifts with a bin width of $z = 0.005$. The red, blue and green lines show the Type Ia, Type II and Type Ib/Ic redshift distributions, respectively. Subtypes (e.g. SN 1991T-like Type Ia supernovae) are included as part of their parent groups. Type Ia supernovae in our sample are predominantly found at higher redshifts, while the Type II supernovae are found at comparatively lower redshifts, as expected from a magnitude-limited sample.

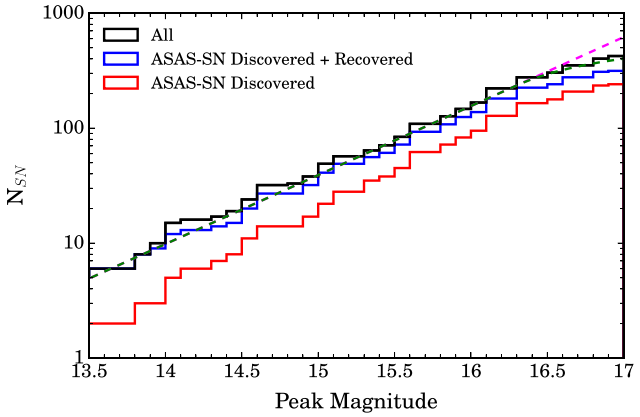

Figure 6. Cumulative histogram of supernovae with respect to peak magnitude, using a 0.1 magnitude bin width. The black line shows the distribution for all supernovae in our sample, while the red line shows only those supernovae discovered by ASAS-SN and the blue line includes both ASAS-SN discoveries and those supernovae that were independently recovered in ASAS-SN data. The green dashed line shows a broken power-law fit normalized to the complete sample assuming a Euclidean slope below the break magnitude and a variable slope for fainter sources, while the lavender dashed line indicates an extrapolation of the Euclidean slope to fainter magnitudes. The fits indicate that the sample is roughly 2/3 complete for $m_{\rm peak} < 17$.

peaking closer to $z \sim 0.03$. This distribution is not unexpected for a magnitude-limited sample, as Type Ia supernovae are typically more luminous than core-collapse supernovae. As was the case in our 2014 sample (see Holoien et al. 2017), the Type Ib/Ic distribution peaks between $z = 0.015$ and $z = 0.02$. This trend is not as clear, due in part to the comparatively small number of Type Ib/Ic supernovae in the sample.

Finally, Fig. 6 shows a cumulative histogram of supernova peak magnitudes with $13.5 < m_{\rm peak} < 17.0$. ASAS-SN discoveries, ASAS-SN discoveries and recovered supernovae and all supernovae from our sample are shown in red, blue and black, respectively. As was the case in the last 8 months of 2014, amateur observers account for a large number of very bright discoveries (those with $m_{\rm peak} \lesssim 14.5$; Holoien et al. 2017). However, in 2015, ASAS-SN discovered a fairly significant fraction of these very bright supernovae as well, showing that it can be competitive with amateurs who observe the relatively small number of very low redshift galaxies with high cadence. ASAS-SN discovers or recovers every supernova with $m_{\rm peak} < 14$, and accounts for a large fraction of the supernovae overall. We discuss the non-recovered cases with $m_{\rm peak} < 15$ in Section 3.2. At $m \sim 16.5$, the distribution flattens, as such supernovae spend less time at magnitudes bright enough to be found by ASAS-SN.

A full discussion of supernova rates is being deferred to an upcoming manuscript (Holoien et al. in preparation), but Fig. 6 illustrates the magnitude completeness of our sample. We fit a broken power law in magnitude (shown with a green dashed line) to the unbinned magnitudes of the theoretically observable SN brighter than $m = 17.0$ assuming a Euclidean slope below the break magnitude and a variable slope for fainter sources, deriving the parameters and their uncertainties using Monte Carlo Markov Chain methods. For the SN discovered by ASAS-SN, the number counts are consistent with a Euclidean slope down to 16.30 ± 0.08 mag, which is about 0.3 mag fainter than we found for the 2013/2014 sample and another indication of improvements in our survey and pipelines. For the samples adding SN later found by ASAS-SN or the sample of all bright SN, we find similar break magnitudes of 16.26 ± 0.07 and 16.27 ± 0.07 mag, respectively.

The integral completenesses of the three samples relative to the Euclidean predictions are 0.95 ± 0.03 (0.64 ± 0.04), 0.93 ± 0.03 (0.60 ± 0.03) and 0.94 ± 0.03 (0.64 ± 0.03) at 16.5 (17.0) mag, respectively. The differential completenesses of the three samples relative to the Euclidean predictions are 0.62 ± 0.09 (0.19 ± 0.05), 0.54 ± 0.06 (0.15 ± 0.03) and 0.60 ± 0.07 (0.20 ± 0.04) at 16.5 (17.0) mag, respectively. These results vary little between the three sample definitions and a rough characterization is that 2/3 of the SN brighter than 17 mag are being found, but only one in 5–6 of the 17 mag SN are being found (relative to the Euclidean extrapolation from the brighter <16 mag SN). The Euclidean approximation modestly underestimates the true completeness for the faint SN because of deviations from a Euclidean geometry, the effects of time dilation on rates and *K*-corrections. We will include these higher order corrections when we carry out a full analysis of the rates.

3.2 Examination of missed cases

In Holoien et al. (2017), we performed a retrospective examination of all bright supernovae that were not discovered or recovered by ASAS-SN in a single month (2014 August) in order to better understand some of the reasons ASAS-SN would not recover supernovae that should be bright enough to be detected. Our conclusion was that many of the missed cases in 2014 would be recovered by ASAS-SN today, due to factors such as better cadence, Galactic plane coverage and an improved detection pipeline.

This is born out in the observations. From 2014 May 1 through 2014 December 31, ASAS-SN recovered 24 per cent (19/80) of the supernovae discovered by other sources. In 2015, this fraction increased dramatically, to 55 per cent (57/104), indicating that our recovery rate has indeed improved since 2014. Of the 47 supernovae that were not recovered, roughly half (23) had peak magnitudes of $m_{\rm peak} \geq 16.5$, which makes them more likely to be missed in our data due to factors such as peaking between ASAS-SN observations or occurring during the full moon, when our survey depth is reduced. While it is clear that there is still room for improvement, ASAS-SN is now recovering more than half of the supernovae discovered by

other supernova searches, and we expect this fraction to continue to increase in the future.

A similar analysis of missed cases to the one performed in Holoien et al. (2017) is unlikely to reveal additional useful information regarding the reasons that ASAS-SN does not recover bright supernovae in our data. We expect that the majority of missed cases in 2015 would have been missed for similar reasons to those discussed in the 2014 catalogue. Instead, here we focus on the very bright ($m_{\rm peak} \leq 15.0$) supernovae from 2015. These are supernovae that should be detectable in ASAS-SN data regardless of observing conditions, and are also the most interesting supernovae for follow-up study due to their brightness. Understanding the reasons why we missed such supernovae is important to ensure that we miss as few of them as possible going forward. Of the supernovae discovered by other professional searches and amateurs in 2015, 13 had $m_{\rm peak} \leq 15.0$. Of these 13, only 2 (SN 2015I and MASTER OT J141023.42−431843.7) were not independently recovered in ASAS-SN data. We examine these two cases in detail here.

SN 2015I was discovered in NGC 2357 on 2015 May 2 by amateur astronomers (CBET 4106), and peaked at a magnitude of 14.0. Unfortunately, the field containing this supernova was not observable due to Sun constraints from either of our telescope sites for a significant portion of 2015: we were unable to observe the field between 2015 April 22 and 2015 August 29. While the host galaxy had not quite set for the season at the time of discovery, our northern unit Brutus is constrained in how far west it is able to observe due to the presence of the LCOGT 2-m telescope in the same enclosure. Since the supernova was discovered at the beginning of this timeframe, it had faded beyond our detection limit by the time we were able to observe it. While it is unfortunate that we were not able to observe this supernova, there is little that could be done to allow us to discover or recover cases like these.

MASTER OT J141023.42−431843.7 was discovered in NGC 5483 on 2015 December 15 by MASTER (Gorbovskoy et al. 2013), and peaked at a magnitude of 14.4. This supernova occurred in an observing field that was transferred to one of the new Cassius cameras in the summer of 2015, when we upgraded our Cassius unit to four telescopes. Before performing image subtraction in a field, we first construct a reference image by co-adding numerous high-quality exposures. Because of weather and technical issues at the start of operations with four cameras, almost no images were obtained in good conditions prior to the field setting in 2015 September. When the field was again observable in 2016 January, the supernova was present, but we did not have enough high-quality images to build a proper reference image. As a result, new images (containing the supernova) would have been rapidly incorporated into the reference image, preventing detection. The supernova faded below our detection limits on 2016 January 16. Essentially, this was a case of bad timing, as the supernova occurred in a field that was not ready for searching at the time it was observable. The field now has a very good reference image built from images spread over the last year, and the supernova is trivially found in multiple epochs if we analyse the data from 2016 January using the current reference image.

While we never want to miss any of the brightest supernovae, neither of these cases was observable by ASAS-SN, and the number of very bright supernovae we have missed has decreased over time: in the latter 8 months of 2014, we missed four supernovae with $m_{\rm peak} \leq 15.0$. This indicates that we have improved our efficiency with very bright supernovae to the point where we are now highly unlikely to miss them in the future if they are observable by ASAS-SN.

4 CONCLUSION

This manuscript provides the second comprehensive catalogue of spectroscopically confirmed bright supernovae and their hosts created by the ASAS-SN team. We now have collected information on 2.5 yr of ASAS-SN discoveries and 20 months of discoveries from other professional surveys and amateurs. The full combined sample comprises 454 supernovae, 271 of which were discovered by ASAS-SN. We also include an analysis of trends with supernova type, location, peak magnitude, sky position and redshift, as well as with host galaxy luminosity and supernova offsets from host nuclei. The analyses suggest that the sample closely resembles that of an ideal magnitude-limited survey as described by Li et al. (2011), but with a smaller-than-expected proportion of Type Ia supernovae relative to core-collapse supernovae.

ASAS-SN remains the only professional survey attempting to provide a complete, all-sky, rapid-cadence survey of the nearby Universe, and as such it has had a significant impact on the discovery and follow-up of bright supernovae in its first 2.5 yr of operation. Even today ASAS-SN operates in a region of parameter space that is largely monitored by amateur astronomers, who focus on bright, nearby galaxies for their supernova searches, and it operates with fewer biases. The analysis presented in this paper indicates that ASAS-SN is finding supernovae that otherwise would not be discovered (e.g. Fig. 3), that it eliminates much of the Northern hemisphere bias in supernova discoveries (Fig. 4) and that it systematically discovers supernovae closer to galactic nuclei than both amateurs and other professionals and in significantly less luminous galaxies than amateurs (Fig. 2). Compared to our performance in 2014 (Holoien et al. 2017), we independently recovered a significantly higher fraction of non-ASAS-SN discoveries in 2015, and we recovered all very bright ($m_{\rm peak} \leq 15.0$) supernovae that were observable by our telescopes in 2015.

The completeness of our full sample has also improved since the end of 2014. In Fig. 6, we show that the magnitude distribution of the bright supernovae discovered between 2014 May 1 and 2015 December 31 is roughly complete to a peak magnitude of $m_{\rm peak} = 16.3$, and is roughly 66 per cent complete for $m_{\rm peak} \leq 17.0$. While we still must address the absolute normalization of the expected number of supernovae (by accounting for factors such as sky coverage and time windows) in order to determine nearby supernovae rates, this analysis serves as a precursor to rate calculations that will be presented in future work by the ASAS-SN team (Holoien et al. in preparation). As noted in Holoien et al. (2017), such nearby rate calculations have the potential to impact a number of fields, including the nearby core-collapse rate (e.g. Horiuchi et al. 2011, 2013) and multimessenger studies ranging from gravitational waves (e.g. Ando et al. 2013; Nakamura et al. 2016), to MeV gamma-rays from Type Ia supernovae (e.g. Horiuchi & Beacom 2010; Diehl et al. 2014; Churazov et al. 2015) to GeV–TeV gamma-rays and neutrinos from rare types of core-collapse supernovae (e.g. Ando & Beacom 2005; Murase et al. 2011; Abbasi et al. 2012). These joint measurements would greatly increase the scientific reach of ASAS-SN discoveries.

This is the second of a yearly series of bright supernova catalogues provided by the ASAS-SN team. It is our hope that by collecting and publishing these data on supernovae and their hosts that we will create convenient and useful repositories that can be used for new and interesting population studies. These catalogues also provide a tool for other professional supernova surveys to perform similar analyses of their data pipelines as we have done for ASAS-SN. While ASAS-SN may discover fewer supernovae than

other professional surveys because it is limited to only bright supernovae, it does find the best and the brightest, and these catalogues are one way in which we can fully leverage the unbiased ASAS-SN sample to impact the field of supernova science now and in the future.

ACKNOWLEDGEMENTS

The authors thank LCOGT and its staff for their continued support of ASAS-SN.

ASAS-SN is supported by NSF grant AST-1515927. Development of ASAS-SN has been supported by NSF grant AST-0908816, the Center for Cosmology and AstroParticle Physics at the Ohio State University, the Mt. Cuba Astronomical Foundation and by George Skestos.

TW-SH is supported by the DOE Computational Science Graduate Fellowship, grant number DE-FG02-97ER25308. JSB, KZS and CSK are supported by NSF grant AST-1515927. KZS and CSK are also supported by NSF grant AST-1515876. BJS is supported by NASA through Hubble Fellowship grant HST-HF-51348.001 awarded by the Space Telescope Science Institute, which is operated by the Association of Universities for Research in Astronomy, Inc., for NASA, under contract NAS 5-26555. Support for JLP is in part provided by FONDECYT through the grant 1151445 and by the Ministry of Economy, Development and Tourism's Millennium Science Initiative through grant IC120009, awarded to The Millennium Institute of Astrophysics, MAS. SD is supported by 'the Strategic Priority Research Program-The Emergence of Cosmological Structures' of the Chinese Academy of Sciences (Grant No. XDB09000000) and Project 11573003 supported by NSFC. JFB is supported by NSF grant PHY-1404311. PRW acknowledges support from the US Department of Energy as part of the Laboratory Directed Research and Development program at LANL.

This research has made use of the XRT Data Analysis Software (XRTDAS) developed under the responsibility of the ASI Science Data Center (ASDC), Italy. At Penn State the NASA *Swift* program is support through contract NAS5-00136.

This research was made possible through the use of the AAVSO Photometric All-Sky Survey (APASS), funded by the Robert Martin Ayers Sciences Fund.

This research has made use of data provided by Astrometry.net (Barron et al. 2008).

This paper uses data products produced by the OIR Telescope Data Center, supported by the Smithsonian Astrophysical Observatory.

Observations made with the NASA *Galaxy Evolution Explorer* (*GALEX*) were used in the analyses presented in this manuscript. Some of the data presented in this paper were obtained from the Mikulski Archive for Space Telescopes (MAST). STScI is operated by the Association of Universities for Research in Astronomy, Inc., under NASA contract NAS5-26555. Support for MAST for non-*HST* data is provided by the NASA Office of Space Science via grant NNX13AC07G and by other grants and contracts.

Funding for SDSS-III has been provided by the Alfred P. Sloan Foundation, the Participating Institutions, the National Science Foundation and the U.S. Department of Energy Office of Science. The SDSS-III web site is http://www.sdss3.org/.

This publication makes use of data products from the Two Micron All Sky Survey, which is a joint project of the University of Massachusetts and the Infrared Processing and Analysis Center/California Institute of Technology, funded by NASA and the National Science Foundation.

This publication makes use of data products from the *Wide-field Infrared Survey Explorer*, which is a joint project of the University of California, Los Angeles and the Jet Propulsion Laboratory/California Institute of Technology, funded by NASA.

This research has made use of the NASA/IPAC Extragalactic Database (NED), which is operated by the Jet Propulsion Laboratory, California Institute of Technology, under contract with NASA.

REFERENCES

Abbasi R. et al., 2012, A&A, 539, A60
Alam S. et al., 2015, ApJS, 219, 12
Ando S., Beacom J. F., 2005, Phys. Rev. Lett., 95, 061103
Ando S. et al., 2013, Rev. Mod. Phys., 85, 1401
Baltay C. et al., 2013, PASP, 125, 683
Barron J. T., Stumm C., Hogg D. W., Lang D., Roweis S., 2008, AJ, 135, 414
Benetti S. et al., 2015, Astron. Telegram, 7040
Blondin S., Tonry J. L., 2007, ApJ, 666, 1024
Brimacombe J. et al., 2015a, Astron. Telegram, 6921
Brimacombe J. et al., 2015b, Astron. Telegram, 6943
Brimacombe J. et al., 2015c, Astron. Telegram, 6950
Brimacombe J. et al., 2015d, Astron. Telegram, 6959
Brimacombe J. et al., 2015e, Astron. Telegram, 6984
Brown T. M. et al., 2013, PASP, 125, 1031
Brown J. S., Shappee B. J., Holoien T. W.-S., Stanek K. Z., Kochanek C. S., Prieto J. L., 2016, MNRAS, 462, 3993
Brown J. S., W.-S Holoien T., Auchettl K., Stanek K. Z., Kochanek C. S., Shappee B. J., Prieto J. L., Grupe D., 2017, preprint (arXiv:1609.04403)
Challis P., Kirshner R., Falco E., 2015a, Astron. Telegram, 6947
Challis P., Kirshner R., Falco E., Calkins M., 2015b, Astron. Telegram, 6956
Chambers K. C. et al., 2016, preprint (arXiv:1612.05560)
Churazov E. et al., 2015, ApJ, 812, 62
Conseil E. et al., 2015, Astron. Telegram, 6934
Diehl R. et al., 2014, Science, 345, 1162
Dong S. et al., 2015a, Astron. Telegram, 6864
Dong S. et al., 2015b, Astron. Telegram, 6886
Dong S. et al., 2015c, Astron. Telegram, 6892
Dong S. et al., 2016, Science, 351, 257
Drake A. J. et al., 2009, ApJ, 696, 870
Dressler A. et al., 2011, PASP, 123, 288
Fabricant D., Cheimets P., Caldwell N., Geary J., 1998, PASP, 110, 79
Fernandez J. M. et al., 2015a, Astron. Telegram, 6983
Fernandez J. M. et al., 2015b, Astron. Telegram, 6989
Fremling C. et al., 2015a, Astron. Telegram, 6909
Fremling C. et al., 2015b, Astron. Telegram, 6974
Frieman J. A. et al., 2008, AJ, 135, 338
Gal-Yam A., Mazzali P. A., Manulis I., Bishop D., 2013, PASP, 125, 749
Godoy-Rivera D. et al., 2017, MNRAS, 466, 1428
Gonzalez C. et al., 2015, Astron. Telegram, 6919
Gorbovskoy E. S. et al., 2013, Astron. Rep., 57, 233
Harutyunyan A. H. et al., 2008, A&A, 488, 383
Herczeg G. J. et al., 2016, ApJ, 831, 133
Hodgkin S. T., Wyrzykowski L., Blagorodnova N., Koposov S., 2013, Phil. Trans. R. Soc. A, 371, 20120239
Holoien T. W.-S. et al., 2014a, MNRAS, 445, 3263
Holoien T. W.-S. et al., 2014b, ApJ, 785, L35
Holoien T. W.-S. et al., 2015a, Astron. Telegram, 6894
Holoien T. W.-S. et al., 2015b, Astron. Telegram, 6990
Holoien T. W.-S. et al., 2016a, Acta Astron., 66, 219
Holoien T. W.-S. et al., 2016b, MNRAS, 455, 2918
Holoien T. W.-S. et al., 2016c, MNRAS, 463, 3813
Holoien T. W.-S. et al., 2017, MNRAS, 464, 2672
Horiuchi S., Beacom J. F., 2010, ApJ, 723, 329
Horiuchi S., Beacom J. F., Kochanek C. S., Prieto J. L., Stanek K. Z., Thompson T. A., 2011, ApJ, 738, 154

Horiuchi S., Beacom J. F., Bothwell M. S., Thompson T. A., 2013, ApJ, 769, 113
Kato T. et al., 2014a, PASJ, 66, 30
Kato T. et al., 2014b, PASJ, 66, 90
Kato T. et al., 2015, PASJ, 67, 105
Kato T. et al., 2016, PASJ, 68, 65
Kiyota S. et al., 2015a, Astron. Telegram, 6870
Kiyota S. et al., 2015b, Astron. Telegram, 6915
Kiyota S. et al., 2015c, Astron. Telegram, 6936
Kiyota S. et al., 2015d, Astron. Telegram, 6945
Kiyota S. et al., 2015e, Astron. Telegram, 6979
Kochanek C. S. et al., 2001, ApJ, 560, 566
Law N. M. et al., 2009, PASP, 121, 1395
Leloudas G. et al., 2016, Nat. Astron., 1, 0002
Li W. D. et al., 2000, in Holt S. S., Zhang W. W., eds, AIP Conf. Ser. Vol. 522, Cosmic Explosions: Tenth Astrophysics Conference. Am. Inst. Phys., New York, p. 103
Li W. et al., 2011, MNRAS, 412, 1441
Martini P. et al., 2011, PASP, 123, 187
Milisavljevic D., Villar V. A., Lunnan R., Drout M., Patnaude D., Berger E., 2015, Astron. Telegram, 6948
Morrell N., Phillips M. M., Contreras C., Busta L., Hsia E. Y., 2015a, Astron. Telegram, 6920
Morrell N. et al., 2015b, Astron. Telegram, 6988
Murase K., Thompson T. A., Lacki B. C., Beacom J. F., 2011, Phys. Rev. D, 84, 043003
Nakamura K., Horiuchi S., Tanaka M., Hayama K., Takiwaki T., Kotake K., 2016, MNRAS, 461, 3296
Nyholm A. et al., 2015, Astron. Telegram, 6994
Ochner P. et al., 2015, Astron. Telegram, 6925
Pastorello A. et al., 2015, MNRAS, 453, 3649
Pignata G. et al., 2009, in Giobbi G., Tornambe A., Raimondo G., Limongi M., Antonelli L. A., Menci N., Brocato E., eds, AIP Conf. Ser. Vol. 1111, Probing Stellar Populations out to the Distant Universe: CEFALU 2008. Am. Inst. Phys, New York, p. 551
Quimby R. M., 2006, PhD thesis, Univ. Texas at Austin
Schlafly E. F., Finkbeiner D. P., 2011, ApJ, 737, 103
Schmidt S. J. et al., 2014, ApJ, 781, L24
Schmidt S. J. et al., 2016, ApJ, 828, L22
Shappee B. J. et al., 2014, ApJ, 788, 48
Shappee B. J. et al., 2015a, Astron. Telegram, 6867
Shappee B. J. et al., 2015b, Astron. Telegram, 6882
Shappee B. J. et al., 2016, ApJ, 826, 144
Simon J., Morrell N., Phillips M. M., 2015, Astron. Telegram, 6905
Skrutskie M. F. et al., 2006, AJ, 131, 1163
Tomasella L. et al., 2015, Astron. Telegram, 6899
Tonry J. L., 2011, PASP, 123, 58
Wright E. L. et al., 2010, AJ, 140, 1868
Wyrzykowski Ł. et al., 2014, Acta Astron., 64, 197
Zhang J., Wang X., 2015a, Astron. Telegram, 6949
Zhang J., Wang X., 2015b, Astron. Telegram, 7006

SUPPORTING INFORMATION

Supplementary data are available at *MNRAS* online.

Table 1. ASAS-SN supernovae.
Table 2. Non-ASAS-SN supernovae.
Table 3. ASAS-SN supernova host galaxies.
Table 4. Non-ASAS-SN supernova host galaxies.

Please note: Oxford University Press is not responsible for the content or functionality of any supporting materials supplied by the authors. Any queries (other than missing material) should be directed to the corresponding author for the article.

[1]*Department of Astronomy, The Ohio State University, 140 West 18th Avenue, Columbus, OH 43210, USA*
[2]*Center for Cosmology and AstroParticle Physics (CCAPP), The Ohio State University, 191 W. Woodruff Ave., Columbus, OH 43210, USA*
[3]*Carnegie Observatories, 813 Santa Barbara Street, Pasadena, CA 91101, USA*
[4]*Núcleo de Astronomía de la Facultad de Ingeniería, Universidad Diego Portales, Av. Ejército 441, Santiago, Chile*
[5]*Millennium Institute of Astrophysics, Santiago, Chile*
[6]*Kavli Institute for Astronomy and Astrophysics, Peking University, Yi He Yuan Road 5, Hai Dian District, Beijing 100871, China*
[7]*Coral Towers Observatory, Cairns, Queensland 4870, Australia*
[8]*Rochester Academy of Science, 1194 West Avenue, Hilton, NY 14468, USA*
[9]*Grove City High School, 4665 Hoover Road, Grove City, OH 43123, USA*
[10]*Department of Physics, The Ohio State University, 191 W. Woodruff Ave., Columbus, OH 43210, USA*
[11]*Astrophysics Research Institute, Liverpool John Moores University, 146 Brownlow Hill, Liverpool L3 5RF, UK*
[12]*Harvard-Smithsonian Center for Astrophysics, 60 Garden St., Cambridge, MA 02138, USA*
[13]*Warsaw University Astronomical Observatory, Al. Ujazdowskie 4, PL-00-478 Warsaw, Poland*
[14]*Los Alamos National Laboratory, Mail Stop B244, Los Alamos, NM 87545, USA*
[15]*Las Campanas Observatory, Carnegie Observatories, Casilla 601, La Serena, Chile*
[16]*Runaway Bay Observatory, 1 Lee Road, Runaway Bay, Queensland 4216, Australia*
[17]*Observatorio Cerro del Viento, MPC I84, Pl. Fernandez Pirfano 3-5A, E-06010 Badajoz, Spain*
[18]*Association Francaise des Observateurs d'Etoiles Variables (AFOEV), Observatoire de Strasbourg, 11 Rue de l'Universite, F-67000 Strasbourg, France*
[19]*Cruz Observatory, 1971 Haverton Drive, Reynoldsburg, OH 43068, USA*
[20]*Observatory Inmaculada del Molino, Hernando de Esturmio 46, Osuna, E-41640 Sevilla, Spain*
[21]*Department of Astronomy, Peking University, Yi He Yuan Road 5, Hai Dian District, Beijing 100871, China*
[22]*Department of Physics, Florida State University, 77 Chieftain Way, Tallahassee, FL 32306, USA*
[23]*Variable Star Observers League in Japan, 7-1 Kitahatsutomi, Kamagaya, Chiba 273-0126, Japan*
[24]*Antelope Hills Observatory, 980 Antelope Drive West, Bennett, CO 80102, USA*
[25]*Roof Observatory Kaufering, Lessingstr. 16, D-86916 Kaufering, Germany*
[26]*Leyburn & Loganholme Observatories, 45 Kiewa Drive, Loganholme, Queensland 4129, Australia*
[27]*Virtual Telescope Project, Via Madonna de Loco, I-47-03023 Ceccano (FR), Italy*
[28]*Kleinkaroo Observatory, Calitzdorp, St. Helena 1B, PO Box 281, 6660 Calitzdorp, Western Cape, South Africa*
[29]*European Southern Observatory, Casilla 19001, Santiago, Chile*
[30]*Mount Vernon Observatory, 6 Mount Vernon Place, Nelson, New Zealand*
[31]*Groupe SNAude France, 364 Chemin de Notre Dame, F-06220 Vallauris, France*
[32]*LBT Observatory, University of Arizona, Tucson, AZ 85721-0065, USA*
[33]*Department of Earth and Environmental Sciences, University of Minnesota, 230 Heller Hall, 1114 Kirby Drive, Duluth, MN 55812, USA*

This paper has been typeset from a TEX/LATEX file prepared by the author.